Case Study

Comparison of Rainfall Interpolation Methods in a Mountainous Region of a Tropical Island

Alan Mair[1] and Ali Fares[2]

Abstract: A total of 21 gauges across the mountainous leeward portion of the island of Oʻahu, Hawaiʻi, were used to compare rainfall interpolation methods and assess rainfall spatial variability over a 34-month monitoring period from 2005 to 2008. Traditional and geostatistical interpolation methods, including Thiessen polygon, inverse distance weighting (IDW), linear regression, ordinary kriging (OK), and simple kriging with varying local means (SKlm) methods were used to estimate wet and dry season rainfall. The linear regression and SKlm methods were used to incorporate two types of exhaustive secondary information: (1) elevation extracted from a digital elevation model (DEM), and (2) distance to a regional rainfall maximum. The Thiessen method produced the highest error, whereas OK produced the lowest error in all but one period. The OK method produced more accurate predictions than linear regression of rainfall against elevation when the correlation between rainfall and elevation is moderate ($R < 0.82$). The SKlm method produced lower error than linear regression and IDW methods in all periods. Comparison of the OK interpolation map with gridded isohyet data indicate that the areas of greatest rainfall deficit were confined to the mountainous region of west Oʻahu. **DOI: 10.1061/(ASCE)HE.1943-5584.0000330.** © 2011 American Society of Civil Engineers.

CE Database subject headings: Rainfall; Spatial analysis; Hawaiʻi; Mountains; Tropical regions; Estimation.

Author keywords: Rainfall; Spatial analysis; Hawaiʻi; Estimation.

Introduction

Assessing the spatial distribution of rainfall is frequently required for water resource management, hydrologic and ecologic modeling, recharge assessment, and irrigation scheduling. In mountainous regions, evaluating rainfall distribution is more complicated because rainfall patterns are influenced by high changes in topographical relief over relatively short distances. The ability to accurately characterize variable rainfall patterns requires a dense network of gauges that involves prohibitive installation and maintenance costs. Hydrologists are frequently required to estimate point rainfall at unrecorded locations from measurements at surrounding sites. Optimizing rain gauge network design and selecting an appropriate interpolation method requires knowledge of rainfall spatial variability.

Traditional approaches for estimating areal and point rainfall have included station-average, Thiessen polygon, inverse distance weighting (IDW), and isohyetal methods (Thiessen 1911; Shepard 1968; McCuen 1989). As an alternative to conventional approaches, geostatistical methods are now used for rainfall estimation. Geostatistics is based on the theory of regionalized variables and provides a set of statistical tools for incorporating the spatial

correlation of observations in data processing (Goovaerts 1997). It is a commonly preferred method because it allows one to account for spatial correlation between neighboring observations to estimate values at ungauged locations. Several studies have found that geostatistics produces better estimates of precipitation than traditional methods (Bacchi and Kottegoda 1995; Christel and Reed 1999; Goovaerts 2000; Campling et al. 2001; Drogue et al. 2002; Buytaert et al. 2006).

Another advantage of geostatistics is that the inclusion of more densely sampled secondary attributes (e.g., weather radar data, elevation) with sparsely sampled measurement of the primary attribute (e.g., rainfall) can be used to improve rainfall estimation. Two multivariate geostatistical methods, ordinary cokriging (OCK) and kriging with an external drift (KED), have been used for merging rain gauge and radar-rainfall data (Creutin et al. 1988; Seo et al. 1990; Raspa et al. 1997). Elevation data have also been merged with rain gauge data to improve rainfall estimation by using these and other geostatistical methods (Hevesi et al. 1992; Christel and Reed 1999; Goovaerts 2000; Sarangi et al. 2005; Carrera-Hernandez and Gaskin 2007). Others have estimated rainfall through a linear regression of rainfall versus elevation, whereas elevation is derived by grid cell from a digital elevation model (DEM) (Daly et al. 1994).

Goovaerts (2000) compared the rainfall prediction performances of two types of interpolation methods: (1) methods that use only rainfall data from 36 stations [Thiessen polygon, IDW, and ordinary kriging (OK)]; and (2) methods that combine rainfall data with elevation [linear regression, SKlm, KED, colocated ordinary cokriging (CCK)]. The largest prediction errors were obtained for the Thiessen polygon and IDW methods. The SKlm method produced the smallest error in most months and yielded the best prediction overall. However, OK produced smaller errors than all other methods when the correlation between rainfall and elevation was less than 0.75. Goovaerts (2000) suggested that other types

[1]Postdoctoral Fellow, Dept. of Geology and Geophysics, and Water Resources Research Center, Univ. of Hawaiʻi at Mānoa, 1689 East-West Road, POST 701, Honolulu, HI 96822 (corresponding author). E-mail: mair@hawaii.edu

[2]Professor, Dept. of Natural Resources and Environmental Management, Univ. of Hawaiʻi at Mānoa, 1910 East-West Rd., Sherman Lab 101, Honolulu, HI 96822. E-mail: afares@hawaii.edu

JOURNAL OF HYDROLOGIC ENGINEERING © ASCE / APRIL 2011 / **371**

J. Hydrol. Eng. 2011, 16(4): 371-383

of secondary information be investigated to assess whether they can further improve rainfall interpolation.

The KED and CCK methods can be cumbersome to apply because of their additional computational complexity and geostatistical software limitations. For example, CCK requires that a linear model of coregionalization be fitted, a feature that is not available in many popular geostatistical software applications (Deutsch and Journel 1998; ESRI 2008; Robertson 2008; Hansen 2010). The wide variety of geostatistical applications and the continuous development of new methods make it difficult to find all the necessary elements in one software for one specific application (Goovaerts 2010). In the case of CCK, the public domain software GSLIB (Deutsch and Journel 1998) is the only geostatistical software of the four previously mentioned that can perform CCK. However, cross-validation is not an option in the existing CCK subroutine, and the user is left to modify other FORTRAN subroutines to conduct error analysis. Finally, most of the 29 main geostatistical software programs also lack a GIS interface (Goovaerts 2010).

Over the past 30 years, rainfall has declined significantly in the upper Mākaha Valley, with the greatest reduction at Mt. Ka'ala, the headwaters area for Mākaha Stream and the highest point on the island of O'ahu (1,227 m) (Mair and Fares 2010a). More rapid warming at higher elevations and increased persistence of the trade wind inversion have also been observed in other parts of Hawai'i over the same period and may be a contributing factor to more rapid rainfall decline at higher elevations (Cao et al. 2007; Giambelluca et al. 2008). The upper Mākaha Valley is part of a much larger preservation district in the Wai'anae Mountains with critical importance for groundwater recharge, irrigation water supply, and protected habitat of endangered native species (Townscape 2009). Thus, investigating the spatial variability of rainfall across the Mākaha Valley and the surrounding area is of renewed interest.

This study examines the spatial variability of rainfall across Mākaha Valley and west O'ahu from 2005 to 2008. The prediction performances of OK and SKlm were compared with other traditional interpolation methods by using cross-validation in a GIS environment. We combined rainfall data with two types of secondary information: (1) elevation derived from the DEM of west O'ahu, and (2) distance to the regional rainfall maximum. Seasonal rainfall data were then interpolated to map the spatial variability. The resulting patterns of rainfall spatial variability were compared with rainfall isohyet maps.

Study Area

The west O'ahu study area comprises an area of 280 km^2 and encompasses most of the Wai'anae Mountains (Fig. 1). The
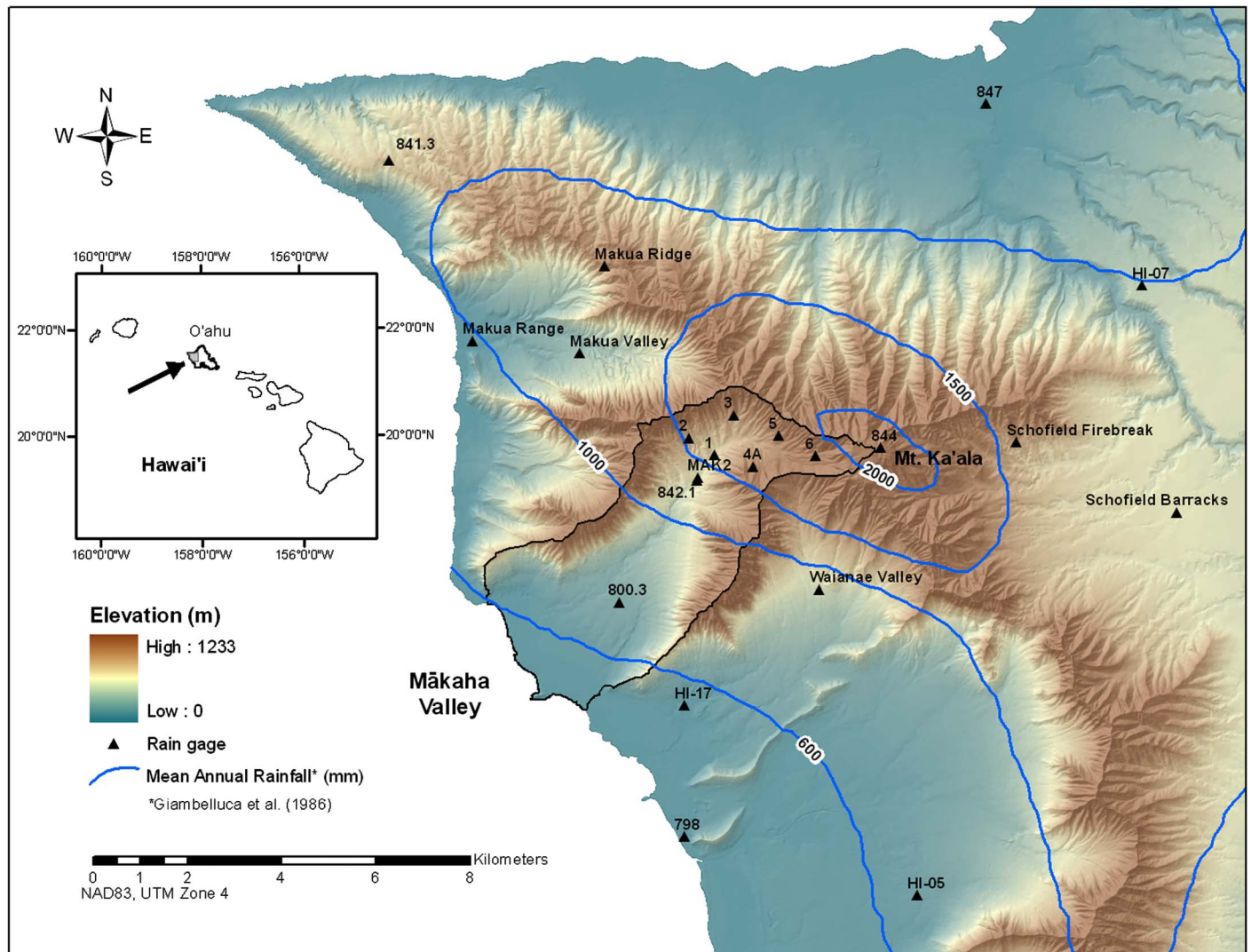

Fig. 1. Location map of west O'ahu, Mākaha Valley, and rain gauges

topography of the area is rugged and varies from sea level to the top of Mt. Ka'ala at 1,226 m. Average annual rainfall varies from 600 mm near the coast to more than 2,000 mm around Mt. Ka'ala (Giambelluca et al. 1986). The long-term monthly and annual rainfall isohyet maps for west O'ahu depict a single, regional maximum around Mt. Ka'ala. The rainfall patterns imply that rainfall diminishes with distance from Mt. Ka'ala in west O'ahu, and that rainfall interpolation might be improved by incorporating this information. Numerous leeward valleys, including the Mākaha Valley, extend from the mountain ridgeline to the sea along the dry leeward coast of O'ahu. Slope along the steep valley walls reaches more than 350%. The Mākaha Valley encompasses a total area of 23.9 km^2, while its upper part comprises an area of only 5.5 km^2.

Before 1976, a total of 1,985 rain gauges operated at one time or another in Hawai'i (0.125 gauges km^{-2}) (Schroeder 1981). The dense gauge network was developed because of large rainfall spatial variability and a need to support plantation agriculture (sugar cane and pineapple) and local water purveyors. Giambelluca et al. (1986) used this network to produce isohyet maps of monthly and annual rainfall for six of the main Hawai'ian Islands, including O'ahu, where the density reached 0.199 gauges km^{-2}. With the decline in plantation agriculture in the 1970s and 1980s, the number of operating gauges diminished by more than 50% on O'ahu by 1993 (0.093 gauges km^{-2}) (Fontaine 1996). However, most of these gauges were located at lower elevations in the central/eastern portions of the island. During this time, a total of nine operating gauges were located in west O'ahu (0.032 gauges km^{-2}), of which only two were located above an elevation of 300 m (0.013 gauges km^{-2}). Over the last 10 years, monitoring by the Desert Research Institute's Western Regional Climate Center (DRI-WRCC) and the University of Hawai'i at Mānoa, Department of Natural Resources and Environmental Management (UHM-NREM) has increased the number of operating gauges in west O'ahu to 23 (0.082 gauges km^{-2}), of which 10 are located above 300 m.

Data Collection and Preprocessing

Daily rainfall data collected from August 2005 to July 2008 at 22 of 23 operating rain gauges were used in this study (Table 1). Data from seven gauges were collected as part of an ongoing research study by UHM-NREM. Data for gauge 842.1 were obtained from the Department of Meteorology (UHM-MET) and the U.S. Geological Survey (USGS) in hard copy and electronic form. Data for 14 other rain gauges were obtained from different online sources, including the National Oceanic and Atmospheric Administration's (NOAA) National Climate Data Center (NCDC), available at http://www.ncdc.noaa.gov/oa/climate/stationlocator.html, NOAA's Hydronet system, available at http://www.prh.noaa.gov/hnl/hydro/hydronet/hydronet-data.php, and DRI-WRCC's Remote Automatic Weather Stations (RAWS), available at http://www.raws.dri.edu/hiF.html. Data from the online sources were collected for the same period except for four of the NCDC gauges, which extend through May 2008. The remaining operating gauge was excluded because of data quality concerns (Dillingham not shown). Gridded rainfall data at a resolution of 250 m and obtained from the rainfall atlas by Giambelluca et al. (1986) were used to obtain the long-term average monthly and annual rainfall at each gauge. The database was provided by T.W. Giambelluca and L. Cuo.

A correction factor of 1.33 was applied to all daily observations collected from 842.1 to adjust measurements affected by tree growth (Mair and Fares 2010b). Missing rainfall data as a percentage of daily measurements were observed in all but two gauges (841.3, Schofield Firebreak) and ranged from 0.1 to 33% over the monitoring period (Table 2). A correlation analysis was used to compile a list of index gauges. Missing daily rainfall values were then estimated by using the normal ratio method and the three most correlated index gauges (Mair and Fares 2010b). In September 2006, MAK2 was installed in a forest clearing 65 m north of 842.1 to assess the effect of tree growth on rainfall catch at 842.1. Therefore, we considered these two gauges as one location

Table 1. Rain Gauge Network

Gauge ID	Lat (°N)/Lat (°W)	Record length	Data source	Zone
1	21°30′23″/158°10′36″	2005–2008	UHM-NREM	High
2	21°30′35″/158°10′55″	2005–2008	UHM-NREM	High
3	21°30′51″/158°10′21″	2005–2008	UHM-NREM	High
4A	21°30′15″/158°10′08″	2006–2008	UHM-NREM	High
5	21°30′36″/158°09′48″	2005–2008	UHM-NREM	High
6	21°30′22″/158°09′22″	2005–2008	UHM-NREM	High
MAK2	21°30′08″/158°10′48″	2006–2008	UHM-NREM	Medium
HI-05	21°25′19″/158°08′08″	1994–2008	NOAA-Hydronet	Low
HI-07	21°32′19″/158°05′20″	1994–2008	NOAA-Hydronet	Medium
HI-17	21°27′31″/158°10′59″	1994–2008	NOAA-Hydronet	Low
798	21°25′60″/158°10′60″	1949–2008	NOAA-NCDC	Low
800.3	21°28′42″/158°11′47″	1987–2008	NOAA-NCDC	Low
841.3	21°34′00″/158°14′00″	1969–2008	NOAA-NCDC	Low
842.1	21°30′06″/158°10′49″	1959–2008	UHM/USGS	Medium
844	21°30′28″/158°08′33″	1965–2008	NOAA-NCDC	High
847	21°34′25″/158°07′14″	1949–2008	NOAA-NCDC	Low
Makua Range	21°31′43″/158°13′34″	1999–2008	WRCC	Low
Makua Ridge	21°32′34″/158°11′56″	1999–2008	WRCC	Medium
Makua Valley	21°31′34″/158°12′15″	1999–2008	WRCC	Medium
Schofield Barracks	21°29′42″/158°04′55″	1999–2008	WRCC	Medium
Schofield Firebreak	21°30′31″/158°06′53″	2000–2008	WRCC	Medium
Wai'anae Valley	21°28′50″/158°09′19″	2003–2008	WRCC	Low

Table 2. Statistical Summary of Monthly Rainfall

Gauge ID	Mean mm	Median mm	Standard deviation mm	Coeff. of variation —	Min mm	Max mm	Elevation m	Distance to regional max m	N Month	N Day	Missing Day	Missing %
MAK2	88	55	64	0.73	20	220	292	2,538	23	700	144	21%
1	108	76	101	0.94	17	565	344	2,136	36	1096	67	6.1%
2	98	67	102	1.05	9	586	477	2,706	36	1096	18	1.6%
3	128	88	124	0.97	17	692	538	1,935	36	1096	17	1.6%
4A	117	73	90	0.77	37	332	610	1,350	23	700	6	0.9%
5	151	94	127	0.84	15	657	605	884	36	1096	224	20%
6	166	112	125	0.75	15	571	731	0	36	1096	77	7.0%
798	39	10	69	1.75	0	369	8	8,548	34	1035	12	1.2%
800.3	43	16	68	1.59	0	363	82	5,198	34	1035	22	2.1%
841.3	62	49	47	0.76	4	228	378	11,010	36	1096	0	0%
842.1	103	64	118	1.14	7	640	286	2,559	36	1096	27	2.5%
844	127	78	114	0.90	19	516	1227	1,395	34	1035	128	12%
847	59	23	92	1.57	0	500	5	8,303	34	1035	339	33%
HI-05	44	21	70	1.60	0	396	35	9,573	36	1096	12	1.1%
HI-07	64	39	79	1.23	0	391	207	7,812	36	1096	12	1.1%
HI-17	37	14	68	1.83	0	387	9	5,979	36	1096	6	0.5%
Makua Range	45	18	58	1.29	2	310	6	7,677	36	1096	162	15%
Makua Ridge	90	56	103	1.14	12	593	534	6,013	36	1096	118	11%
Makua Valley	81	51	83	1.03	9	414	159	5,457	36	1096	334	30%
Schofield Barracks	65	33	100	1.53	5	584	299	7,772	36	1096	27	2.5%
Schofield Firebreak	81	45	103	1.26	5	498	347	4,282	36	1096	0	0%
Wai'anae Valley	65	29	84	1.30	6	446	292	2,838	36	1096	1	0.1%

for the purposes of the spatial analysis. Data from 842.1 were used in the analysis from August 2005 to August 2006, whereas data from MAK2 were used from September 2006 to July 2008. Gauge 4A was added to the network in September 2006. Thus, the operating west Oʻahu rain gauge network for this study consisted of 20 gauges from August 2005 to August 2006, and 21 gauges from September 2006 to July 2008 (Fig. 1).

Rainfall data were aggregated into a monthly format to produce a 36-month-long time series extending from August 2005 to July 2008. The time series of monthly rainfall data were reviewed and then compiled into seasonal wet and dry periods to examine the differences in rainfall distribution. Rainfall data were also grouped into a water year extending from October 1 to September 30 to keep winter and summer seasonality intact. Given the incomplete records for water years 2005 and 2008, annualized rainfall data consisted of water years 2006 and 2007 only. Two types of exhaustive secondary information, elevation and distance to the regional rainfall maximum, were used for rainfall interpolation. Elevation was extracted from a DEM of Oʻahu with a grid size of 10 m and obtained online from NOAA's Center for Coastal Monitoring and Assessment website available at http://ccma.nos.noaa.gov/. A second set of secondary information was computed a posteriori as the linear distance from the location of the regional rainfall maximum to each respective gauge. The location of the regional rainfall maximum was selected as the gauge with maximum rainfall over each of the aggregation periods. The distance from the regional rainfall maximum was determined by using the same grid cells depicted in the DEM.

Interpolation Methods

A brief description of the rainfall interpolation methods used to estimate rainfall depth at unsampled locations is described

subsequently. These include Thiessen polygon, IDW, linear regression, OK, and SKlm. For more detailed descriptions of these methods, the reader is referred to Goovaerts (1997, 2000). The geostatistical analysis extension module of ArcEditor 9.3.1 (ESRI 2008), and GS+ v. 9 (Robertson 2008) were used to aid the analyses and generate rainfall spatial variability maps. The set of rainfall data was measured at $n = 20$ locations (before September 1, 2006) and $n = 21$ (after September 1, 2006).

Thiessen polygons is a simple and straightforward method whereby each unsampled or interpolated location is given the value of the closest observation (Thiessen 1911). For the IDW method, the value at each interpolated location is estimated as a linear combination of surrounding observations, with the weights being inversely proportional to the distance between the observations and the interpolated location (Shepard 1968). We used an optimal value of b, a constant by which the distance is weighted, that resulted in the lowest error. A total of 14 observations were used for the IDW method. Next, consider the situation where rainfall data are supplemented by secondary information, available at all primary attribute locations. The rainfall depth at the interpolated location can be estimated by using a linear regression between rainfall and the colocated secondary information. Linear regression models are contingent on assumptions of linearity between dependent and independent variables, constant variance of the errors, and normality of the error distribution. The assumption of normality for primary, secondary, and residual data was tested by using the Kolmogorov-Smirnov test (McCuen 2003; SAS 2010).

Kriging is a term used by geostatisticians for a family of generalized least-squares regression methods that use available data in a specified search neighborhood to estimate the values at unsampled locations (Isaaks and Srivastava 1989; Goovaerts 1997; Deutsch and Journel 1998). Let $\{z(\mathbf{u}_\alpha), \alpha = 1, ..., n\}$ be the set of rainfall data measured at $n = 20$ locations (before September 1,

2006) and $n = 21$ (after September 1, 2006). The unknown values $z(\mathbf{u})$ and data values $z(\mathbf{u}_\alpha)$ are interpreted as realizations of random variables (RVs) $Z(\mathbf{u})$ and $Z(\mathbf{u}_\alpha)$. All versions of kriging are variations of the basic generalized linear regression method and estimator $Z^*(\mathbf{u})$ as follows (Deutsch and Journel 1998)

$$Z^*(\mathbf{u}) - m(\mathbf{u}) = \sum_{\alpha=1}^{n(\mathbf{u})} \lambda_\alpha(\mathbf{u})[z(\mathbf{u}_\alpha) - m(\mathbf{u}_\alpha)] \qquad (1)$$

where $\lambda_\alpha(\mathbf{u})$ = kriging weight assigned to the datum $z(\mathbf{u}_\alpha)$. The parameters $m(\mathbf{u})$ and $m(\mathbf{u}_\alpha)$ are the expected values of $Z(\mathbf{u})$ and $Z(\mathbf{u}_\alpha)$, respectively. In practice, only $n(\mathbf{u})$ data within a given window $W(\mathbf{u})$ centered on $\mathbf{u}$ are included in the estimation.

All types of kriging methods strive to minimize the estimation variance, $\sigma_E^2(\mathbf{u})$, with the constraint of unbiasedness of the estimator as follows:

$$\sigma_E^2(\mathbf{u}) = \text{Var}[Z^*(\mathbf{u}) - Z(\mathbf{u})], \qquad E[Z^*(\mathbf{u}) - Z(\mathbf{u})] = 0 \qquad (2)$$

where $\text{Var}[Z^*(\mathbf{u}) - Z(\mathbf{u})]$ = estimation variance and $E[Z^*(\mathbf{u}) - Z(\mathbf{u})]$ = expected error. The RV $Z(\mathbf{u})$ is decomposed into a residual component $R(\mathbf{u})$ and a trend component or expected value $m(\mathbf{u})$

$$Z(\mathbf{u}) = R(\mathbf{u}) + m(\mathbf{u}) \qquad (3)$$

where $R(\mathbf{u})$ is modeled as a stationary random function (RF) with zero mean and covariance $C(\mathbf{h})$.

Geostatistics uses the semivariogram $\gamma(\mathbf{h})$ as a measure of dissimilarity between observations. The experimental semivariogram $\hat{\gamma}(\mathbf{h})$ is computed as half the average squared difference between the components of data pairs

$$\hat{\gamma}(\mathbf{h}) = \frac{1}{2N(\mathbf{h})} \sum_{\alpha=1}^{N(\mathbf{h})} [z(\mathbf{u}_\alpha) - z(\mathbf{u}_\alpha + \mathbf{h})]^2 \qquad (4)$$

where $N(\mathbf{h})$ = number of pairs of data locations a vector $\mathbf{h}$ apart. The semivariogram can account for direction-dependent variability; however, we only computed the omnidirectional semivariogram because of the sparse nature of our sample network. For this study, we chose the widely used spherical semivariogram model for rainfall and elevation because it is characterized by linear behavior at the origin (Goovaerts 2000) and is also a commonly available semivariogram model in many geostatistical software packages (Deutsch and Journel 1998; ESRI 2008; Robertson 2008). The spherical model may be written as

$$\gamma(\mathbf{h}) = \begin{cases} S\left[1.5\frac{\mathbf{h}}{a} - 0.5\left(\frac{\mathbf{h}}{a}\right)^3\right] & \mathbf{h} \le a \\ S & \mathbf{h} \ge a \end{cases} \qquad (5)$$

where $\gamma(\mathbf{h})$ = the spherical semivariogram with range a and sill S for lag distance $\mathbf{h}$.

OK allows one to account for local variation of the mean by limiting the domain of stationarity of the mean to the search neighborhood centered on the interpolated location. The constant but unknown local mean can be removed from the generalized kriging algorithm [Eq. (1)] by forcing the kriging weights to sum to 1. Thus, the OK estimator $Z_{\text{OK}}^*(\mathbf{u})$ may be rewritten as a linear combination only of $n(\mathbf{u})$ RVs $z(\mathbf{u}_\alpha)$

$$Z_{\text{OK}}^*(\mathbf{u}) = \sum_{\alpha=1}^{n(\mathbf{u})} \lambda_\alpha^{\text{OK}}(\mathbf{u})z(\mathbf{u}_\alpha), \qquad \sum_{\alpha=1}^{n(\mathbf{u})} \lambda_\alpha^{\text{OK}}(\mathbf{u}) = 1 \qquad (6)$$

For OK, the kriging weights $\lambda_\alpha^{\text{OK}}(\mathbf{u})$ are determined to minimize the estimation variance and ensure the unbiasedness of the

estimator [Eq. (2)]. These weights may be obtained by solving a system of linear equations as follows:

$$\sum_{\beta=1}^{n(\mathbf{u})} \lambda_\beta^{\text{OK}}(\mathbf{u})\gamma(\mathbf{u}_\alpha - \mathbf{u}_\beta) - \mu^{\text{OK}}(\mathbf{u}) = \gamma(\mathbf{u}_\alpha - \mathbf{u}) \quad \alpha = 1, \dots, n(\mathbf{u})$$

$$\sum_{\beta=1}^{n(\mathbf{u})} \lambda_\beta^{\text{OK}}(\mathbf{u}) = 1 \qquad (7)$$

where $\mu^{\text{OK}}(\mathbf{u})$ = Lagrange parameter accounting for the constraint on the weights.

The SKlm method involves substituting the known stationary mean $m(\mathbf{u})$ in the generalized kriging method in Eq. (1) with the varying means estimator $m_{\text{SK}}^*(\mathbf{u})$ derived from secondary information. One can write the SKlm estimator $Z_{\text{SKlm}}^*(\mathbf{u})$ as the sum of the regression estimate $f(y(\mathbf{u}))$ and the simple kriging estimate of the residual value at $\mathbf{u}$

$$Z_{\text{SKlm}}^*(\mathbf{u}) = f[y(\mathbf{u})] + \sum_{\alpha=1}^{n(\mathbf{u})} \lambda_\alpha^{\text{SK}}(\mathbf{u})r(\mathbf{u}_\alpha)$$

$$r(\mathbf{u}_\alpha) = z(\mathbf{u}_\alpha) - m_{\text{SK}}^*(\mathbf{u}_\alpha) \qquad (8)$$

where $r(\mathbf{u}_\alpha)$ = residual of the observed value $z(\mathbf{u}_\alpha)$ minus the regression estimate, $f[y(\mathbf{u}_\alpha)] = m_{\text{SK}}^*(\mathbf{u}_\alpha)$, at location $\mathbf{u}_\alpha$; and $\lambda_\alpha^{\text{SK}}(\mathbf{u})$ are the kriging weights. Values for $\lambda_\alpha^{\text{SK}}(\mathbf{u})$ are obtained by solving the simple kriging system

$$\sum_{\beta=1}^{n(\mathbf{u})} \lambda_\beta^{\text{SK}}(\mathbf{u})C_R(\mathbf{u}_\alpha - \mathbf{u}_\beta) = C_R(\mathbf{u}_\alpha - \mathbf{u}), \qquad \text{for } \alpha = 1, \dots, n(\mathbf{u})$$

$$(9)$$

where $C_R(\mathbf{h})$ = covariance function of the residual RF, $R(\mathbf{u}) = Z(\mathbf{u}) - m(\mathbf{u})$. If the residuals are uncorrelated such that all the kriging weights in Eq. (8) are zero, the SKlm estimate reduces to the linear regression estimate.

The best spherical semivariogram model was generated by observing the coefficient of determination (R^2) and residual sum square (RSS) values with a trial-and-error approach for different lag sizes and lag intervals (Goovaerts 1997). The lag sizes and number of lags varied because of a general rule of thumb, in which the lag size times the number of lags should be less than one-half of the largest distance between data pairs (Johnston et al. 2010). The optimum model parameters (sill, nugget, and range) corresponding to the highest R^2 value were noted. The performance of the interpolation methods were evaluated and compared by using cross-validation (Isaaks and Srivastava 1989). The method consists of temporarily removing one observation at a time from the data set and reestimating the removed value from the remaining data by using each interpolation method. For this study, the root mean squared error (RMSE) was used as the error criterion for comparison of the model-predicted results with the observed values. The RMSE is defined as

$$\text{RMSE} = \left\{\frac{1}{n} \sum_{\alpha=1}^{n} [z(\mathbf{u}_\alpha) - z^*(\mathbf{u}_\alpha)]^2\right\}^{1/2} \qquad (10)$$

where $z^*(\mathbf{u}_\alpha)$ = reestimated value at location $\mathbf{u}_\alpha$. The RMSE indicates how closely the interpolation method predicts the measured values; hence, the smaller the RMSE, the better the prediction capability. For linear regression, the RMSE was computed as the average residual value for the linear model, which means that the prediction error would tend to be underestimated. To further

JOURNAL OF HYDROLOGIC ENGINEERING © ASCE / APRIL 2011 / **375**

J. Hydrol. Eng., 2011, 16(4): 371-383

assess the performance of each method, the RMSE-observations standard deviation ratio (RSR) was used as an error index (Moriasi et al. 2007).

Results

Mean monthly rainfall over the 36-month monitoring period varied from a low of 37 mm at Gauge HI-17 to a high of 166 mm at Gauge 6 (Table 2). The greatest variability (coefficient of variation > 1.5) was exhibited by gauges with a mean less than 65 mm and located most distant from the mountain ridgeline (798, 800.3, 847, HI-05, HI-17, Schofield Barracks). Rain gauges were split into low, medium, and high rainfall zones according to the long-term average annual rainfall isohyet map (Giambelluca et al. 1986): (1) < 1,000 mm, (2) 1,000–1,500 mm, (3) > 1,500 mm (Fig. 1, Table 1). Gauge measurements within each zone were averaged for comparison. The monthly data display a seasonal pattern in all three zones, consisting of a dry season extending from April to September and a wet season extending from October to March (Fig. 2). However, the pattern was not exclusive, as one of the driest months recorded for the entire period occurred in December 2005. The wettest month occurred in March 2006, when an average of 485 mm was recorded in the gauge network. March 2006 ranked among the wettest months on record at long-term Gauges 842.1 (7th) and 844 (17th). As expected, rainfall accumulation is lowest in the low rainfall zone that consists of gauges most distant from Mt. Ka'ala and closest to the coast and is highest in the high-rainfall zone of the upper Mākaha Valley and Mt. Ka'ala, the dominant local topographic feature (Fig. 2). A similar pattern of rainfall accumulation is evident in all three zones and suggests that all of west O'ahu has a similar rainfall regime that is consistent with the designation by Diaz et al. (2005).

The maximum monthly rainfall was recorded in the upper Mākaha Valley at Gauges 3, 5, and 6 during 33 months of the 36-month monitoring period. Gauge 6 recorded the maximum a total of 25 months and was second highest for eight of the remaining 11 months. The other maxima were recorded along the northern

ridgeline of the Wai'anae Mountains at Mākua Ridge and 841.3. Gauge 844 located atop Mt. Ka'ala was conspicuously missing from the group of gauges with maximum monthly recorded rainfall. Long-term monthly and annual rainfall isohyets all depict a rainfall maximum centered around Mt. Ka'ala (Giambelluca et al. 1986). However, our results suggest that the rainfall maximum occurs northwest of Mt. Ka'ala and leeward of the summit of the ridgeline in the upper Mākaha Valley that is consistent with the pattern of maximum rainfall for mountains situated beneath the cloud base in Hawai'i (Lau and Mink 2006). For this study, we identified Gauge 6 as the location of the regional rainfall maximum. The linear distance to Gauge 6 was then computed for the remaining gauges in the network and recorded as the distance to the regional maximum (Table 2).

The average correlation between monthly rainfall at a lag of one month is 0.76 and declines only slightly to 0.72 at a lag of six months (Fig. 3). The moderate degree of correlation among the
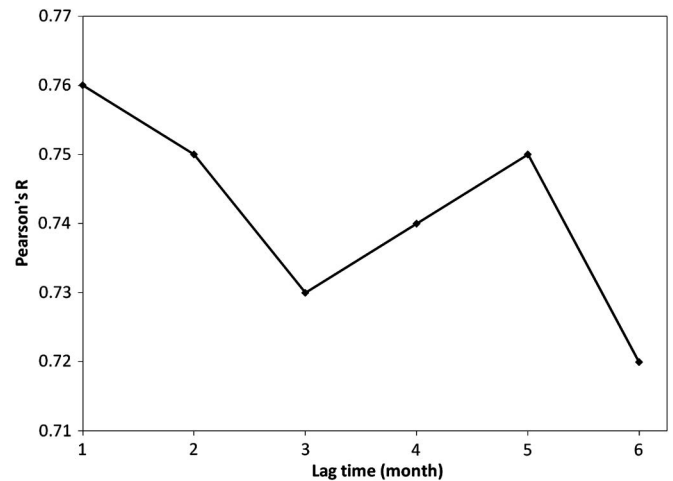

Fig. 3. Average correlation among monthly rainfall data measured at increasing time intervals: 1–6 months
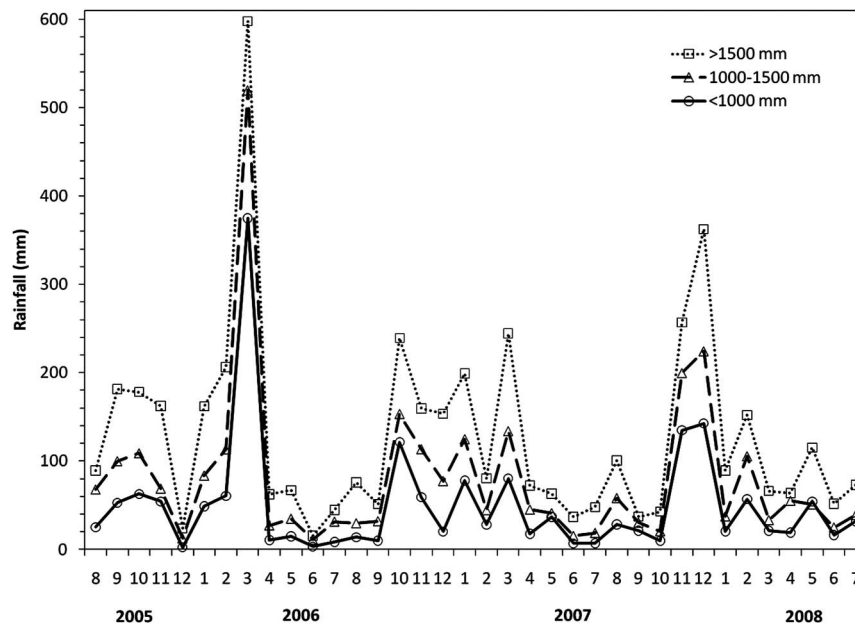

Fig. 2. Average recorded monthly rainfall of rain gauges located within three rainfall zones from August 2005 to July 2008; low, medium, and high rainfall zones are defined by the annual long-term average isohyet map of Giambelluca et al. (1986): < 1,000 mm (low); 1,000–1,500 mm (medium), and > 1,500 mm (high)
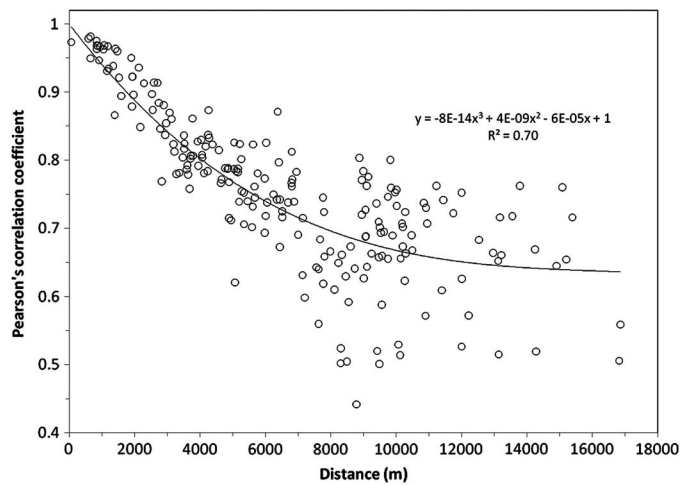
Fig. 4. Spatial correlation of daily rainfall among rain gauges used in this study with a third-order polynomial trendline

Fig. 5. Average seasonal rainfall by rainfall zone (low, medium, high) expressed as a fraction of average long-term rainfall; rainfall zones comprised of $< 1{,}000$ mm, $1{,}000$–$1{,}500$ mm, and $> 1{,}500$ mm

monthly rainfall data is evidence of some topographic control on spatial structure. The spatial correlogram of daily rainfall data indicates that rain gauges at a mutual distance of less than 2,500 m are strongly correlated (Pearson's $R = 0.85$–0.98) (Fig. 4). At distances larger than 2,500 m, the correlation gradually range widens with increasing lag distance ($R = 0.44$–0.87) and indicates that the correlation is less dependent on the actual distance. The correlogram suggests a spatial rainfall distribution characterized by localized topoclimates generated from differences in proximity and location relative to the mountain ridgeline and Mt. Ka'ala. Despite high correlation, cumulative rainfall across short distances can differ significantly. For example, Gauges 1 and 5 are located at a mutual distance of only 1.4 km and show strong correlation in daily rainfall ($R = 0.96$). However, the mean monthly rainfall at Gauge 5 is 40% greater than the mean at Gauge 1 (Table 2). Thus, rainfall tends to accumulate simultaneously (daily time step) at Gauges 1 and 5, but the differences in topography (altitude, distance to
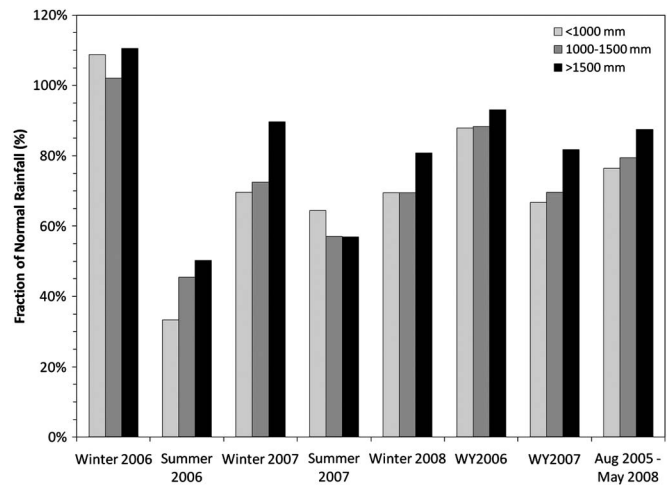
ridgeline) result in a systematic bias in the total amount of rainfall recorded at each rain gauge.

Monthly rainfall data were aggregated into a wet winter season (October to March) and a dry summer season (April to September), annual water years for 2006 and 2007, and total rainfall over the monitoring period (August 2005 to May 2008). For example, the period from October 2005 to March 2006 corresponds to winter 2006. We chose to use seasonally aggregated data to investigate differences in wet and dry season rainfall accumulation in Mākaha Valley and the surrounding area. In addition, the presence of numerous months with no rainfall at multiple gauges precluded the use of geostatistical methods on a monthly time scale. The months of June and July 2008 were excluded from the seasonal spatial analysis because of a lack of data for four of the five NCDC rain gauges (798, 800.3, 844, 847).

Table 3. Descriptive Statistics for Rainfall and Secondary Data

Parameter	N (gauges)	Mean	Median	Standard deviation	Coeff. of variation	Min	Max	Data normality (p-value)	Correlation (R)		Residual normality (p-value)	
									Elev.	Dist.	Elev.	Dist.
Rainfall												
Winter 2006	20	913	839	345	0.38	538	1,545	0.05	0.77	−0.81	> 0.15	> 0.15
Summer 2006	20	169	144	130	0.77	14	479	> 0.15	0.82	−0.68	0.07	> 0.15
Winter 2007	21	691	661	337	0.49	277	1,356	> 0.15	0.75	−0.86	> 0.15	> 0.15
Summer 2007	21	224	206	122	0.55	50	514	> 0.15	0.72	−0.76	> 0.15	> 0.15
Winter 2008	21	648	619	297	0.46	241	1,381	> 0.15	0.81	−0.78	> 0.15	> 0.15
2006	20	1082	940	464	0.43	555	1,971	0.02	0.80	−0.79	> 0.15	> 0.15
2007	21	915	844	454	0.50	344	1,870	0.10	0.75	−0.84	> 0.15	> 0.15
Aug 2005– May 2008	20	2,883	2,569	1,322	0.46	1,327	5,805	0.11	0.80	−0.82	> 0.15	> 0.15
Secondary data												
Elevation	20/21	329/343	296/299	305/304	0.93/0.89	4	1,227	> 0.15/ > 0.15	—	−0.64/ −0.66	—	—
Distance to Max	20/21	5,103/ 4,924	5,328/ 5,198	3,198/ 3,223	0.63/0.65	0	11,010	> 0.15/ 0.11	−0.64/ −0.66	—	—	—

Note: Units = mm for rainfall and m for secondary data.

Seasonal data confirm a strong wet and dry season trend across the area. Winter or wet season rainfall accounted for 84% of regional average rainfall in 2006 and 76% of the regional average in 2007 (Table 3). Greater variability (CV > 0.5) is exhibited during the dry summer months where appreciable amounts of rainfall are generally confined to the high rainfall zone. Gauges in the low rainfall zone (< 1,000 mm annually) commonly recorded little or no rainfall for extended periods during the dry summer season.

Seasonal and annual rainfall are positively correlated with elevation ($R = 0.72$ to 0.82) and negatively correlated with distance to Gauge 6 ($R = -0.68$ to -0.86). Seasonal and annual rainfall data and colocated secondary data are normally distributed at a 5% significant level, except for rainfall from winter 2006 and water year 2006. Residuals from linear regression analyses of rainfall with both elevation and distance to the regional rainfall maximum are all normally distributed. The linear relationship between primary
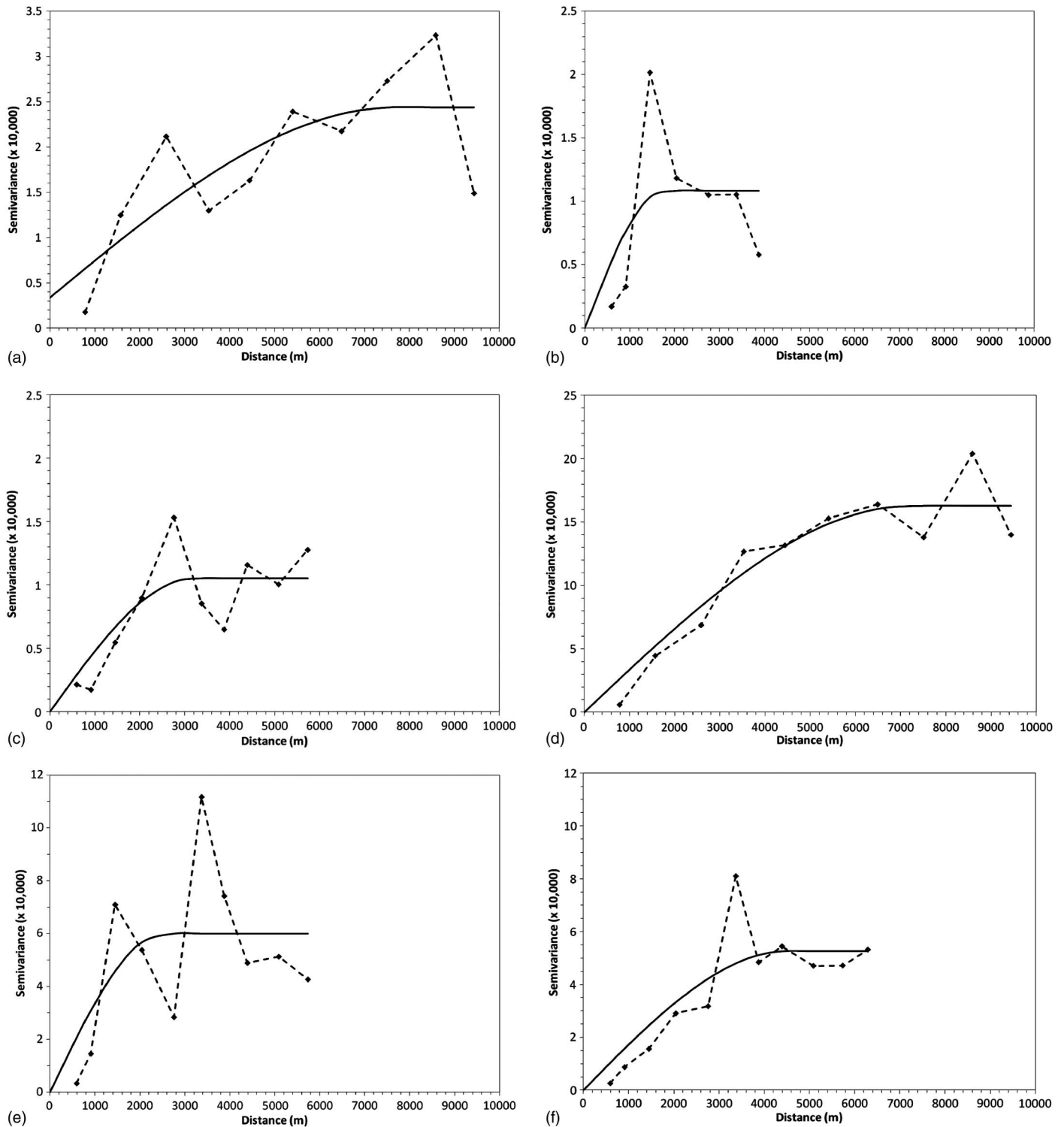
Fig. 6. Semivariograms for seasonal data: (a) rainfall, summer 2006, $R^2 = 0.58$; (b) elevation residuals, summer 2006, $R^2 = 0.43$; (c) distance residuals, summer 2006, $R^2 = 0.68$; (d) rainfall, winter 2006, $R^2 = 0.89$; (e) elevation residuals, winter 2006, $R^2 = 0.40$; (f) distance residuals, winter 2006, $R^2 = 0.76$

and secondary data for all time periods including winter 2006 and water year 2006 and the normal error distribution for all residuals indicates that linear regression is valid for these distributions.

Seasonal rainfall recorded in all three zones was less than the long-term average, except for winter 2006 (Fig. 5). Winter 2006 recorded rainfall at 102–111% of long-term averages, largely a result of high rainfall in March 2006. The greatest departures from long-term averages were recorded during the summer when rainfall was only 33–50% of average in 2006 and 57–64% of average in 2007. Over the 34-month monitoring period, recorded rainfall was only 76–87% of the long-term average for this same period in the three zones. In general, the gauges in the two drier zones experienced greater departures from long-term average rainfall than the gauges from wettest zone. Gauge 844 reported only 73% of the long-term average for the 34-month period, which represents the greatest departure from long-term normal rainfall among gauges in the wettest zone.

For rainfall, the best-fit semivariogram was obtained by using a lag size of 1 km and a total of 10 lag intervals. For residuals, the best-fit semivariogram was obtained by using a lag size of 600 m and seven- to 10-lag intervals for residuals. Semivariogram parameters including nugget, sill, and range and cross-validation statistics were estimated for each wet and dry season, water year

Fig. 7. Predicted versus observed rainfall for ordinary kriging and simple kriging with varying local means methods: (a) summer 2006; (b) winter 2007; predicted values were computed by using cross-validation technique of temporarily removing one observation at a time from the data set and reestimating the removed value from the remaining data

(2006 and 2007), and for the entire 34-month monitoring period (Table 4). Experimental semivariograms of rainfall resulted in R^2 values ranging from 0.58 in summer 2006 to 0.89 in winter 2006 and were consistently more than R^2 values for both residuals, semivariograms (Fig. 6). Cross-validation values of R^2 for OK ranged from a low of 0.67 in summer 2006 to a high of 0.90 in winter 2007 (Fig. 7), while corresponding values of R^2 for SKlm were lower in all cases except summer 2006 (elevation only). The summer of 2006 was extremely dry, and rainfall from this period showed the greatest correlation with elevation and the lowest correlation with distance to the regional maximum among all periods. The relative nugget effect is greater in summer 2006 and reflects greater increasing noise in rainfall data resulting from measurement errors (Goovaerts 2000). The semivariograms of residuals both show a greater range of spatial correlation in winter 2006 when compared to summer 2006 (Fig. 6). Although the range of spatial correlation varies from season to season, there does not appear to be a clear trend of a consistently shorter correlation range in summer than in winter (Table 4). The semivariograms of elevation residuals consistently show a shorter range of correlation than residuals of distance to the regional maximum.

A comparison of prediction errors for all the interpolation methods is expressed as proportions of the RMSE for the OK approach (Fig. 8). Thus, absolute values of the traditional methods can be easily obtained by multiplying these proportions by the RMSE values listed in Table 4. The largest RMSE is produced by the Thiessen polygon method that ignores secondary information. The OK method produces lower RMSE than all other methods except during summer 2006. The correlation between elevation and rainfall was moderately strong ($R = 0.82$) during the summer 2006 period, which suggests that OK yields less prediction error than linear regression when the correlation is smaller than 0.82. Despite strong correlation between the distance to the regional maximum and rainfall ($R = -0.86$), linear regression against distance consistently produces more error than OK. These results suggest that the threshold for better performance of linear regression against distance versus OK requires a correlation greater than -0.86. The SKlm method consistently performed better than linear regression and IDW methods across all time periods. Thus, SKlm is preferable to linear regression and IDW when exhaustive secondary information is available for this network. The greater volatility in relative RMSE when using elevation as compared with distance to the regional maximum (SKlm, linear regression) suggests that elevation may be a less stable form of secondary information for interpolating rainfall in west Oʻahu.

Moriasi et al. (2007) presented performance ratings for the RSR error index and noted that model performance can be considered very good if RSR ≤ 0.50, good if RSR ≤ 0.60, satisfactory if RSR ≤ 0.70, and unsatisfactory if RSR > 0.70. The RSR for the Thiessen polygon, IDW, linear regression against elevation, and linear regression against distance methods ranged from 0.75–0.92, 0.59–0.71, 0.56–0.67, and 0.53–0.72, respectively. Thus, linear regression against elevation was the only nongeostatistical method that produced satisfactory or better results for all time periods. For the geostatistical methods, the range of the RSR improved to satisfactory or better levels, indicating better overall performance than traditional methods (Table 4). Cross-validation indicates that all three geostatistical methods underpredicted and overpredicted observations by amounts equal to or greater the observed value (Fig. 7). However, despite large errors for selected observations, the range of RSR for all three geostatistical methods indicates satisfactory to very good performance overall.

The dramatic difference between the interpolation methods is reflected in the maps of interpolated rainfall for winter 2008
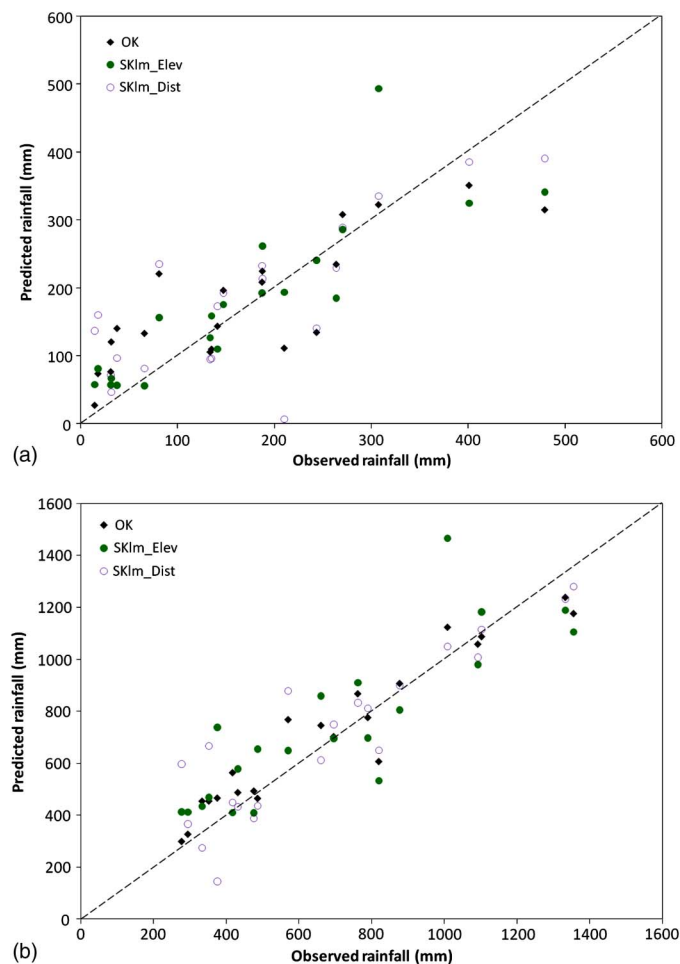
JOURNAL OF HYDROLOGIC ENGINEERING © ASCE / APRIL 2011 / **379**

J. Hydrol. Eng., 2011, 16(4): 371-383

Table 4. Model Fitting, Cross-Validation, and Semivariogram Parameters

Parameter	Semivariogram model				Cross-validation		
	R^2	Nugget (mm^2)	Sill (mm^2)	Range (m)	R^2	RMSE	RSR
Ordinary kriging							
Winter 2006	0.89	100	162,700	7,220	0.76	170.1	0.49
Summer 2006	0.58	3,390	24,390	7,680	0.67	75.0	0.58
Winter 2007	0.84	100	177,800	9,140	0.90	122.2	0.36
Summer 2007	0.70	10	24,130	8,920	0.70	67.5	0.55
Winter 2008	0.74	1,800	133,500	7,930	0.71	162.5	0.55
2006	0.87	100	304,700	7,240	0.81	205.2	0.44
2007	0.81	1,000	328,000	9,090	0.88	172.2	0.38
Aug 2005–May 2008	0.74	1,000	2,478,000	7,630	0.87	505.6	0.38
Simple kriging with varying local means (elevation)							
Winter 2006	0.40	100	59,900	2,540	0.76	174.4	0.51
Summer 2006	0.43	10	10,830	1,774	0.74	66.3	0.51
Winter 2007	0.55	100	60,530	2,233	0.71	184.7	0.55
Summer 2007	0.62	10	10,860	2,424	0.60	79.1	0.65
Winter 2008	0.48	100	43,550	1,928	0.70	164.3	0.55
2006	0.51	100	123,900	2,412	0.79	220.4	0.47
2007	0.70	100	129,200	2,414	0.70	255.8	0.56
Aug 2005–May 2008	0.51	1,000	997,000	1,950	0.75	665	0.50
Simple kriging with varying local means (distance to regional maximum)							
Winter 2006	0.76	100	52,680	4,520	0.72	183	0.53
Summer 2006	0.68	10	10,520	3,200	0.59	82.3	0.63
Winter 2007	0.64	100	34,300	2,660	0.81	143.7	0.43
Summer 2007	0.71	10	6,873	3,270	0.63	74.3	0.61
Winter 2008	0.49	100	33,670	2,660	0.68	165	0.55
2006	0.87	100	102,700	4,490	0.72	244.7	0.53
2007	0.72	100	68,910	2,930	0.77	208.1	0.46
Aug 2005–May 2008	0.81	1,000	688,200	3,580	0.77	635.5	0.48

(Fig. 9), the period when differences in relative RMSE are the least. While the Thiessen method displays the characteristic polygonal zones of influence around the 21 gauges, the IDW method ($b = 4.8$) produces a map with boundaries that appear similar to the Thiessen map. The linear regression approach that uses the two types of secondary information (elevation, distance to regional

Fig. 8. Relative root mean square error (RMSE) of prediction by season, water year, and entire 34-month monitoring period; results are expressed as proportions of the prediction error of the ordinary kriging method

maximum) produces maps that are significantly different from one another despite similar prediction errors. A major limitation of these regressions is that rainfall at a particular location is derived only from the secondary information, regardless of the records at the surrounding rain gauges. The SKlm map that uses elevation does not appear dramatically different from linear regression except where gauge density is high, such as the upper Mākaha Valley. The short range of spatial correlation of SKlm by using elevation results in little or no adjustment to large areas of the linear regression map. The SKlm map that uses distance represents a significant change from linear regression except in the southeast and north central portion of west Oʻahu, where the network is sparse. The OK method produces a map that provides a reasonable representation of rainfall patterns in Mākaha Valley and the adjacent areas where the rain gauge density is greater. However, the OK method struggles to represent patterns clearly in areas where there are few rain gauges, such as the southeast portion of west Oʻahu.

The consistent pattern of a rainfall maximum west of Mt. Kaʻala implies that the upper Mākaha Valley is receiving proportionally greater amounts of rainfall than indicated by the spatial structure of long-term isohyet maps. Annual long-term rainfall data for gauges in the upper valley (1, 2, 3, 5, and 6) and Mt. Kaʻala (844) extracted from gridded isohyet rainfall data suggest that the upper valley receives between 75 and 96% of rainfall recorded at Mt. Kaʻala. However, the results of our 34-month study indicate that these same locations received between 79 and 135% of rainfall recorded at Mt. Kaʻala. We compared the long-term average rainfall map obtained from the gridded rainfall data with the OK map for
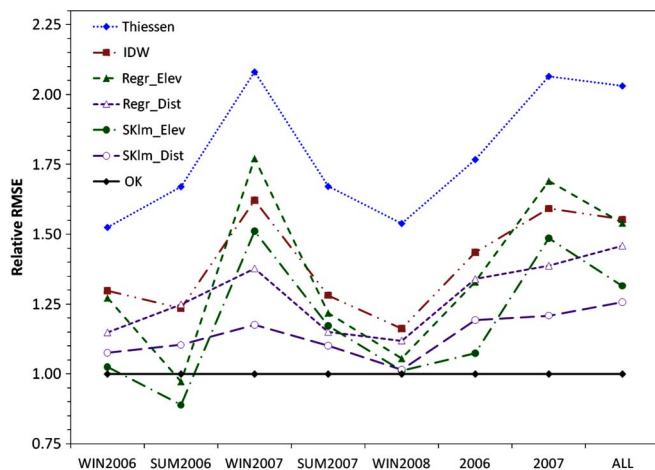
the 34-month period to further investigate the differences in spatial distribution. The gridded rainfall data clearly show a rainfall maximum at Mt. Ka'ala with anisotropic variation centered along the northwest-southeast trend of the northern portion of the Wai'anae Mountain ridgeline [Fig. 10(a)]. Similar to earlier results, the OK map suggests that the wettest area occurs west of Mt. Ka'ala and largely within the upper Mākaha Valley [Fig. 10(b)]. Thus, these results suggest that long-term isohyet maps that show a rainfall maximum around Mt. Ka'ala may need to be adjusted to reflect a rainfall maximum centered west of Mt. Ka'ala and within the upper Mākaha Valley.

The difference between these two maps suggests that most of west O'ahu received less than the long-term average rainfall for this period [Figs. 10(c) and 10(d)]. The greatest differences occurred in the area east-southeast of Mt. Ka'ala, where spatially interpolated rainfall was more than 1,800 mm below or 51–65% of the long-term average. A small area to the west along the Makua coast also received substantially less rainfall than long-term averages. Most of the areas that show the greatest difference from long-term averages (i.e., drier conditions) are located at higher elevations, which is consistent with greater observed reduction in long-term rainfall at higher elevations over the past 30 years (Mair and Fares 2010a). The lack of rain gauge data in the southeast portion of west O'ahu makes it difficult to assess whether the computed differences from long-term averages are valid or merely a reflection of low gauge density in this area. Despite the aforementioned dry conditions, two areas received more than long-term average rainfall: (1) the southern perimeter of the upper Mākaha Valley, and (2) a portion to the north along the Waialua coastline. The above-average rainfall in the upper Mākaha Valley is likely
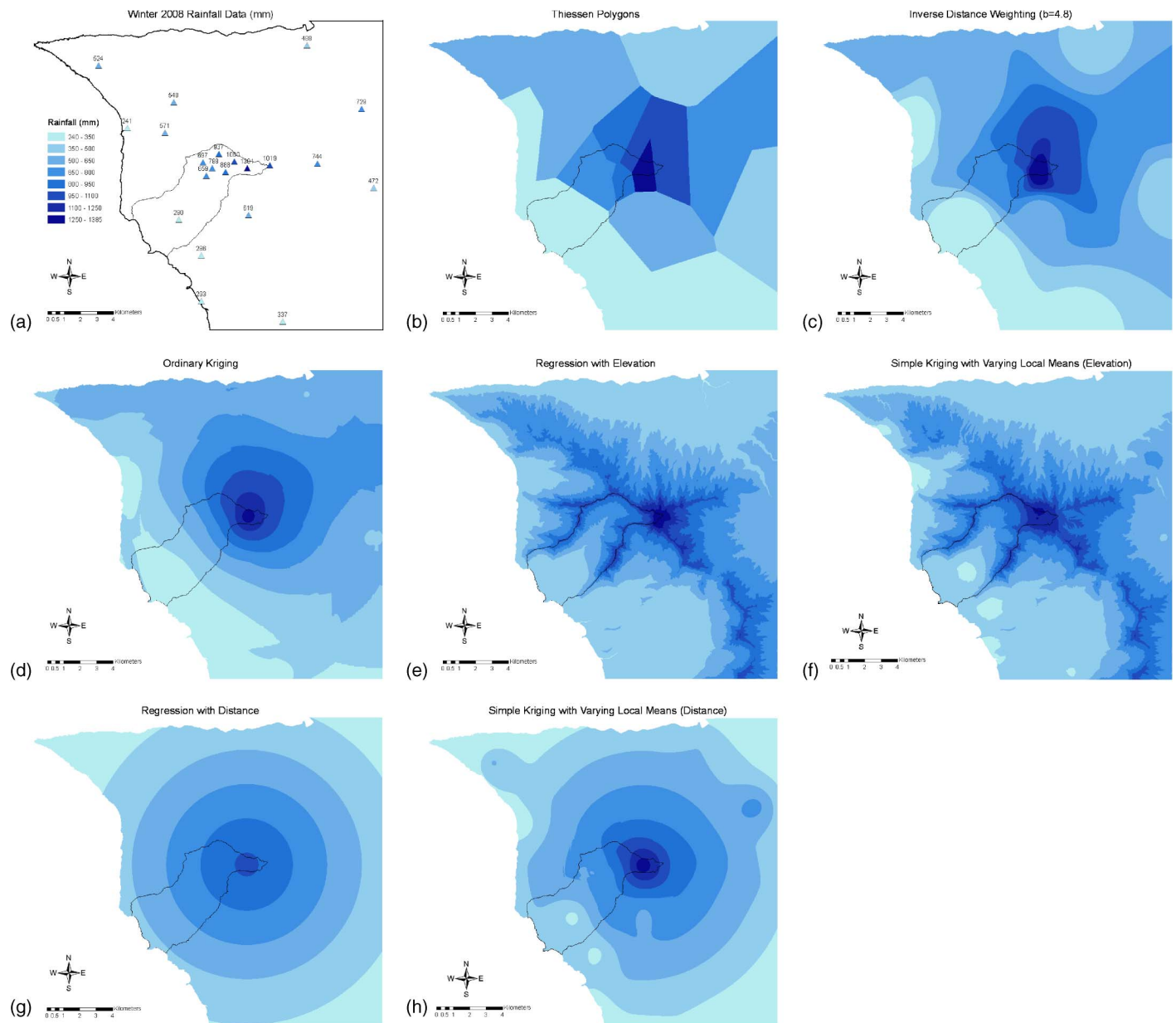

Fig. 9. Winter 2008 rainfall maps obtained by the interpolation of 21 observations: (a) observations; (b) Thiessen polygon; (c) inverse distance weighted ($b = 4.8$); (d) ordinary kriging; (e) linear regression of rainfall with elevation; (f) simple kriging with varying local means by using elevation; (g) linear regression with distance to the regional rainfall maximum; (h) simple kriging with varying local means by using distance to the regional rainfall maximum
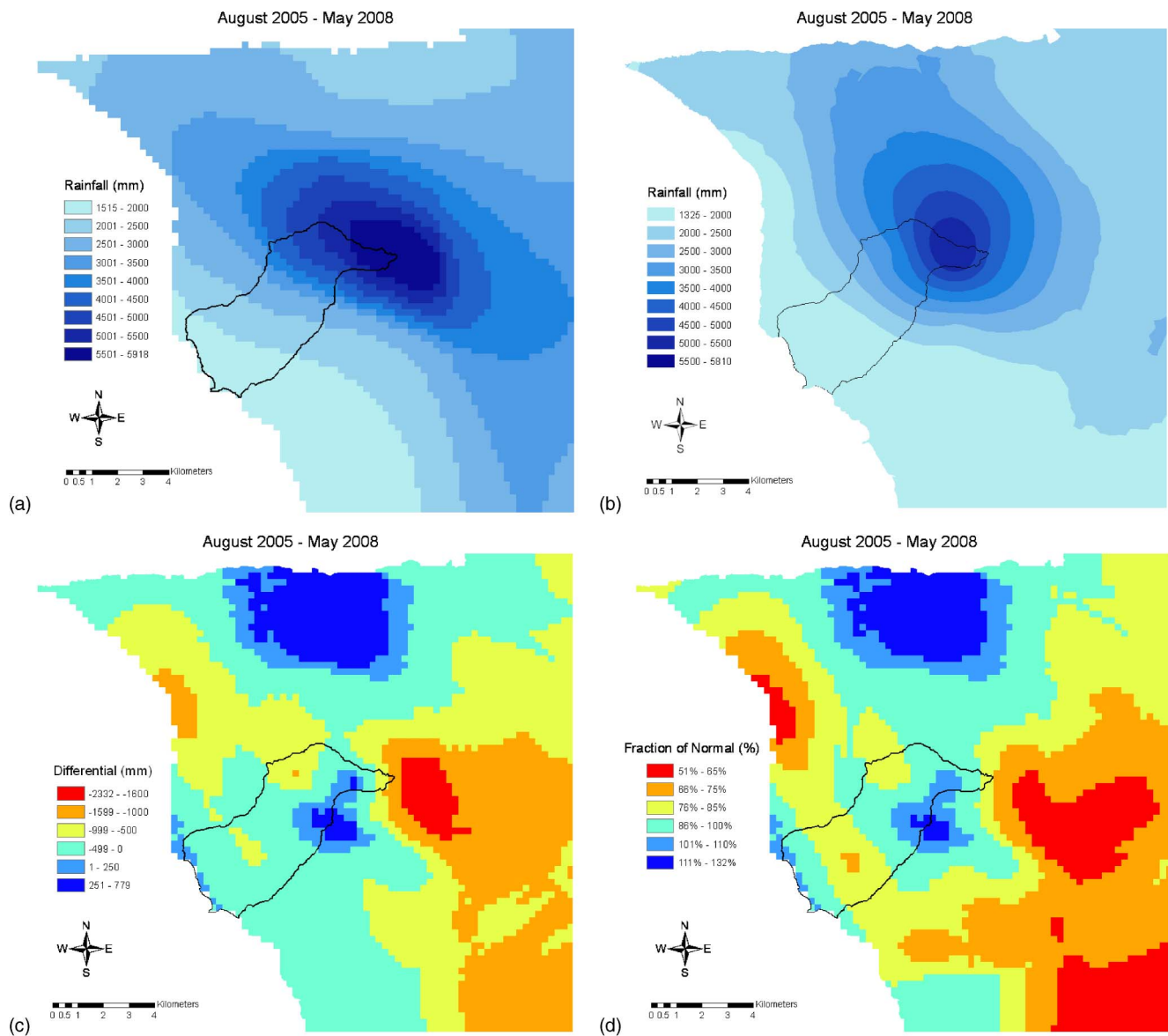
Fig. 10. (a) Gridded rainfall isohyet data for August 2005 to May 2008; (b) rainfall interpolation map obtained by ordinary kriging for August 2005 to May 2008; (c) difference between gridded rainfall data and ordinary kriging map; (d) ordinary kriging map expressed as a fraction of gridded rainfall isoyhet data

attributable to the location of the rainfall maximums, and may not actually reflect above-average rainfall in the area.

Conclusions

Rainfall data recorded from 2005 to 2008 from a network of 21 gauges located across west O'ahu were analyzed to compare rainfall interpolation methods and investigate patterns of spatial variability. Rainfall occurs in a distinct seasonal pattern, consisting of a wet winter season from October to March and a dry summer season from April to September. Wet seasonal rainfall accounts for 76–84% of annual rainfall. Results indicate that the local monthly, seasonal, and annual rainfall maximum consistently occurs in the upper Mākaha Valley located west of Mt. Ka'ala and leeward of the Wai'anae Mountain's ridgeline. The location of the rainfall maximum in Mākaha Valley is contrary to long-term isohyet maps that show a consistent maximum at Mt. Ka'ala. Long-term isohyet maps

may need to be adjusted to reflect the location of a regional maximum west of Mt. Ka'ala.

Traditional methods (Thiessen, IDW, regression) were compared with geostatistical methods (OK, SKlm) for rainfall interpolation. Exhaustive secondary information (elevation, distance to the regional rainfall maximum) were used to improve estimates. The Thiessen polygon method produced the highest prediction error while OK produced the lowest error across all but one time period. The SKlm method outperformed linear regression and IDW methods in all time periods. Our results confirm prior findings (Goovaerts 2000) that geostatistical interpolation (i.e., OK) outperforms traditional methods that ignore the pattern of spatial dependence. However, the incorporation of secondary information did not improve prediction accuracy over OK except when the correlation between rainfall and elevation reached 0.82. Despite a correlation as strong as −0.86 between rainfall and distance to the regional maximum, OK consistently outperformed SKlm and linear regression.

Comparison of an OK interpolation map to gridded long-term isohyet data for the entire 34-month period indicates that the area east-southeast of Mt. Ka'ala received well below-average rainfall (51–65% of normal). The driest areas during the monitoring period are generally confined to higher elevations, which is consistent with the more rapid rainfall decline observed at higher elevations in the Wai'anae Mountains over the previous 30 years. The lack of rain gauge data for the southeast portion of west O'ahu, particularly at higher elevations, makes it difficult to assess spatial variability in that area. The addition of a rain gauge in the southern Wai'anae Mountains would help minimize uncertainty in rainfall spatial variability.

Acknowledgments

References

Bacchi, B., and Kottegoda, N. T. (1995). "Identification and calibration of spatial correlation patterns of rainfall." *J. Hydrol. (Amsterdam, Neth.)*, 165, 311–348.

Buytaert, W., Celleri, R., Willems, P., De Beivre, B., and Wyseure, G. (2006). "Spatial and temporal rainfall variability in mountainous areas: A case study from the south Ecuadorian Andes." *J. Hydrol. (Amsterdam, Neth.)*, 329, 413–421.

Campling, P., Gobin, A., and Feyen, J. (2001). "Temporal and spatial rainfall analysis across a humid tropical catchment." *Hydrol. Processes*, 15, 359–375.

Cao, G., Giambelluca, T. W., Stevens, D. E., and Schroeder, T. A. (2007). "Inversion variability in the Hawaiian trade wind regime." *J. Clim.*, 20, 1145–1160.

Carrera-Hernandez, J. J., and Gaskin, S. J. (2007). "Spatio temporal analysis of daily precipitation and temperature in the basin of Mexico." *J. Hydrol. (Amsterdam, Neth.)*, 336, 231–249.

Christel, P., and Reed, D. W. (1999). "Mapping extreme rainfall in a mountainous region using geostatistical techniques: A case study in Scotland." *Int. J. Climatol.*, 19, 1337–1356.

Creutin, J. D., Delrieu, G., and Lebel, T. (1988). "Rain measurement by rain gage-radar combination: a geostatistical approach." *J. Atmos. Ocean. Technol.*, 5, 102–115.

Daly, C., Neilson, R. P., and Phillips, D. L. (1994). "A statistical topographic model for mapping climatological precipitation over mountainous terrain." *J. Appl. Meteorol.*, 33, 140–158.

Deutsch, C. V., and Journel, A. G. (1998). *GSLIB, Geostatistical software library and user's guide*, 2nd Ed., Oxford University Press, Oxford, UK.

Diaz, H. F., Chu, P.-S., and Eischeid, J. K. (2005). "Rainfall changes in Hawaii during the last century." *16th Conf. on Climate Variability and Change*, San Diego.

Drogue, G., Humbert, J., Deraisme, J., Mahrb, N., and Freslonc, N. (2002). "A statistical-topographic model using an omni-directional parameterization of the relief for mapping orographic rainfall." *Int. J. Climatol.*, 22, 599–613.

ESRI, Inc. (2008). *ArcEditor 9.3.1* [Computer software]. Redlands, CA.

Fontaine, R. A. (1996). "Evaluation of the surface water quantity, surface water quality, and rainfall data collection programs in Hawaii, 1994." *U.S. Geological Survey Water Resources Investigations Rep. 95-4212*, 125–126.

Giambelluca, T. W., Diaz, H. F., and Luke, M. S. A. (2008). "Secular temperature changes in Hawai'i." *Geophys. Res. Lett.*, 35, L12702.

Giambelluca, T. W., Nullet, M. A., and Schroeder, T. A. (1986). "Rainfall atlas of Hawai'i." *Rep. R76*, Dept. of Land and Natural Resources, Honolulu, 267.

Goovaerts, P. (1997). *Geostatistics for natural resources evaluation*, Oxford University Press, New York.

Goovaerts, P. (2000). "Geostatistical approaches for incorporating elevation into the spatial interpolation of rainfall." *J. Hydrol. (Amsterdam, Neth.)*, 228, 113–129.

Goovaerts, P. (2010). "Geostatistical software." *Handbook of applied spatial analysis: Software tools methods and applications*, M. M. Fischer and A. Getis, eds., Springer-Verlag, Berlin, 129–138.

Hansen, T. M. (2010). *mGstat, v. 0.97, a geostatistical Matlab toolbox*, Lyngby, Denmark.

Hevesi, J. A., Istok, J. D., and Flint, A. L. (1992). "Precipitation estimation in mountainous terrain using multivariate geostatistics. Part I: Structural analysis." *J. Appl. Meteorol.*, 31, 661–676.

Isaaks, E. H., Srivastava, R. M. (1989). *An introduction to applied geostatistics*, Oxford University Press, New York.

Johnston, K., Ver Hoef, J. M., Krivoruchko, K., and Lucas, N. (2001). *Using ArcGIS Geostatistical Analyst*, ESRI, Redlands, CA.

Lau, L. S., and Mink, J. F. (2006). *Hydrology of the Hawaiian Islands*, Univ. of Hawai'i Press, Honolulu.

Mair, A. and Fares, A. (2010a). "Influence of groundwater pumping and rainfall spatio-temporal variation on streamflow." *J. Hydrol. (Amsterdam, Neth.)*, 393(3–4), 287–308.

Mair, A., and Fares, A. (2010b). "Assessing rainfall data homogeneity and estimating missing records in Mākaha Valley, O'ahu, Hawai'i." *J. Hydrol. Eng.*, 15, 61–66.

McCuen, R. H. (1989). *Hydrologic analysis and design*, Prentice-Hall, Englewood Cliffs, NJ.

McCuen, R. H. (2003). *Modeling hydrologic change: Statistical methods*, Lewis, Boca Raton, FL.

Moriasi, D. N., Arnold, J. G., Van Liew, M. W., Bingner, R. L., Harmel, R. D., and Veith, T. L. (2007). "Model evaluation guidelines for systematic quantification of accuracy in watershed simulations." *Trans. ASABE*, 50, 885–900.

Raspa, G., Tucci, M., and Bruno, R. (1997). "Reconstruction of rainfall fields by combining ground rain gauges data with radar maps using external drift method." *Geostatistics Wollongong '96*, E. Y. Baafi and N. A. Schofield, eds., Kluwer Academic, Dordrecht, The Netherlands.

Robertson, G. P. (2008). *GS+: Geostatistics for the environmental sciences*, Gamma Design Software, Plainwell, MI.

Sarangi, A., Cox, C. A., and Madramootoo, C. A. (2005). "Geostatistical methods for prediction of spatial variability of rainfall in a mountainous region." *Trans. ASABE*, 48, 943–954.

SAS, Inc. (2010). *Enterprise Guide 4.3* [Computer software], Carey, NC.

Schroeder, T. A. (1981). "A revised precipitation climatology of the Hawaiian islands." *4th Conf. of Hydrometeorology*, Reno, NV.

Seo, D. J., Krajewski, W. F., Azimi-Zonooz, A., and Bowles, D. S. (1990). "Stochastic interpolation of rainfall data from rain gages and radar using cokriging. II. Results." *Water Resour. Res.*, 26, 915–924.

Shepard, D. (1968). "A two-dimensional interpolation function for irregularly-spaced data." *Association for Computing Machinery 23rd Annual Conf.*, ACM, New York.

Thiessen, A. H. (1911). "Precipitation averages for large areas." *Mon. Weather Rev.*, 39, 1082–1089.

Townscape, Inc. (2009). *Wai'anae watershed management plan, pre-final draft prepared for Honolulu Board of Water Supply*, Honolulu.